Supporting Information for

Brightness and AIEE Behaviour of Methylenebis(4,1-phenylene) Linkage Electron Donor-Acceptor-based Dyad and Its Implications for Robust Quantification of Explosive Picric Acid in both Aqueous Medium and Solid State

Manas Mahato[a], Tuhina Sultana[a], Rajkumar Sahoo[b], Sabbir Ahamed[a], Najmin Tohora[a], Arpita Maiti[a] and Sudhir Kumar Das[a]*

[a]Department of Chemistry, University of North Bengal, Raja Rammohunpur, Darjeeling, West Bengal-734013, India

[b]Department of Chemistry, Indian Institute of Technology, Kharagpur, West Bengal-721302, India

Corresponding author: (Dr. S. K. Das; E-mail: sudhirkumardas@nbu.ac.in)

S1: Synthesis procedure of MBH

At first desalted pyridoxal hydrochloride by a simple neutralization method. For this purpose, pyridoxal hydrochloride is stirred with an equivalent amount of potassium hydroxide (KOH) for 3 h to get the resulting pyridoxal. 4,4'-methylenediamine (50 mg, 0.252 mmol) was added to 3-hydroxy-5-(hydroxymethyl)-2-methylisonicotinaldehyde (pyridoxal) (0.504 mmol, 84.24 mg) in 3 mL of MeOH with the following addition of a catalytic amount of acetic acid and then refluxed for 8 h. TLC was used to monitor the progress of the reaction. After condensation, the reaction mixture was cooled, and orange colored solid was filtered and washed systematically with MeOH, after which it was dried in a desiccator. Yield: 91%

Characterizations: ^{1}H NMR (400 MHz, DMSO-d_6, 25 °C) δ(ppm): 13.98 s, (1H, -OH), 9.16 s, (1H, -CH=N), 7.98 s, (1H), 7.46 d, (1H), 7.41 d, (1H), 5.43 s, (1H, -OH), 4.77 d, (1H), 4.06 s, (1H), 2.42 s, (1H, -CH_3), (**Fig. S1**). ^{13}C NMR (100 MHz, δ (ppm), DMSO-d_6): 161.21, 153.61, 148.62, 145.77, 141.66, 138.52, 134.12, 130.37, 122.34, 122.14, 120.32, 58.79, 19.18

(**Fig. S2**) and the mass spectra m/z is found to be 497.2198 (**Fig. S3**) confirming the formation of our **MBH.**

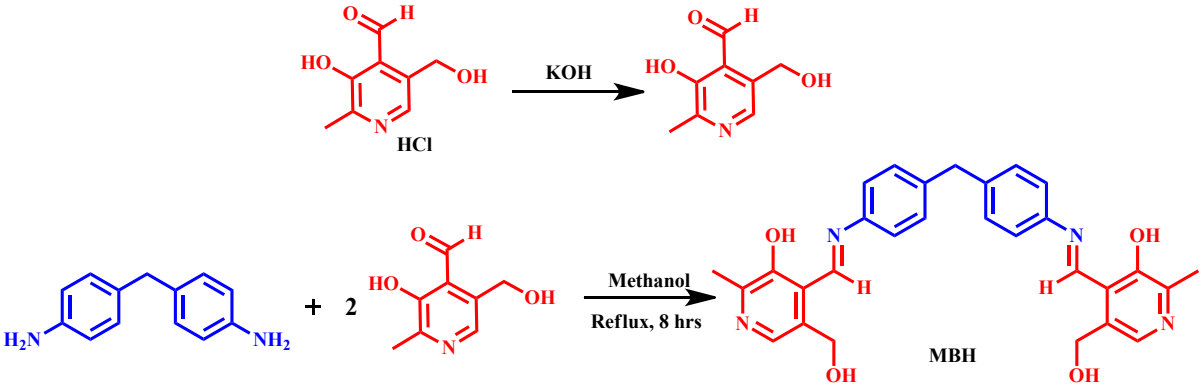

Scheme S1: Synthetic procedure of our desired probe **MBH.**

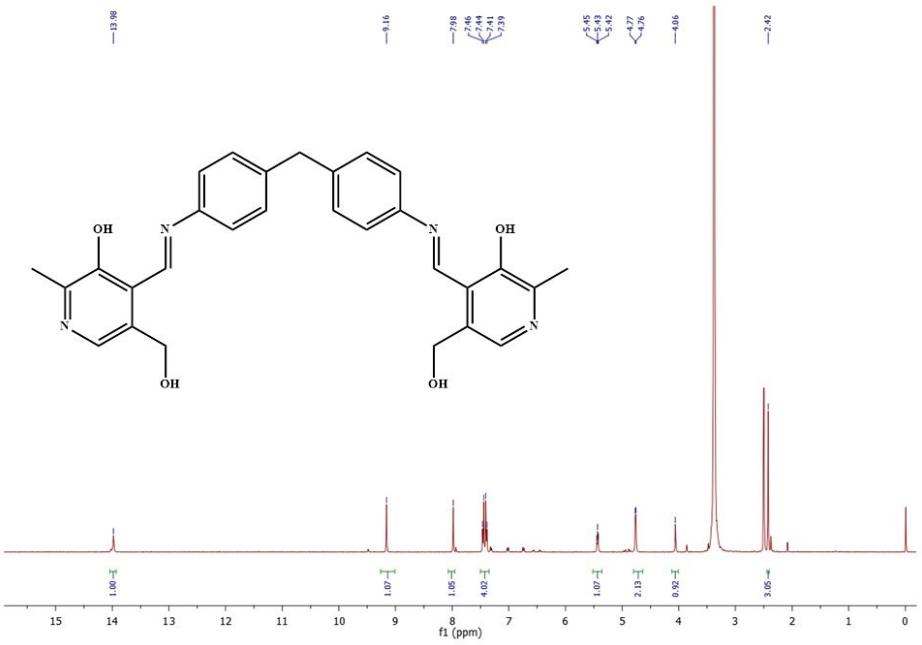

Fig. S1 ^{1}H NMR of probe **MBH.**

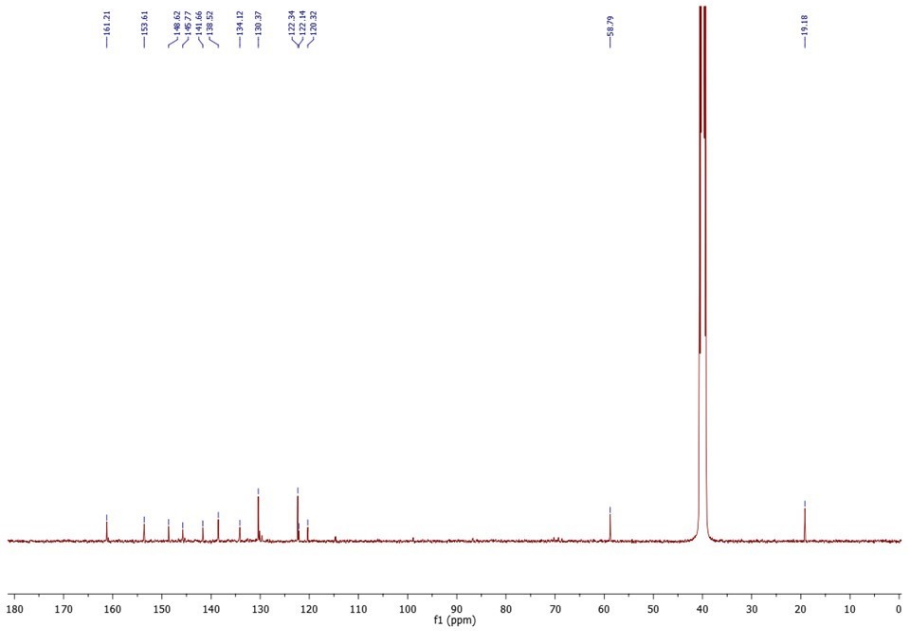

Fig. S2 ^{13}C NMR of probe **MBH.**

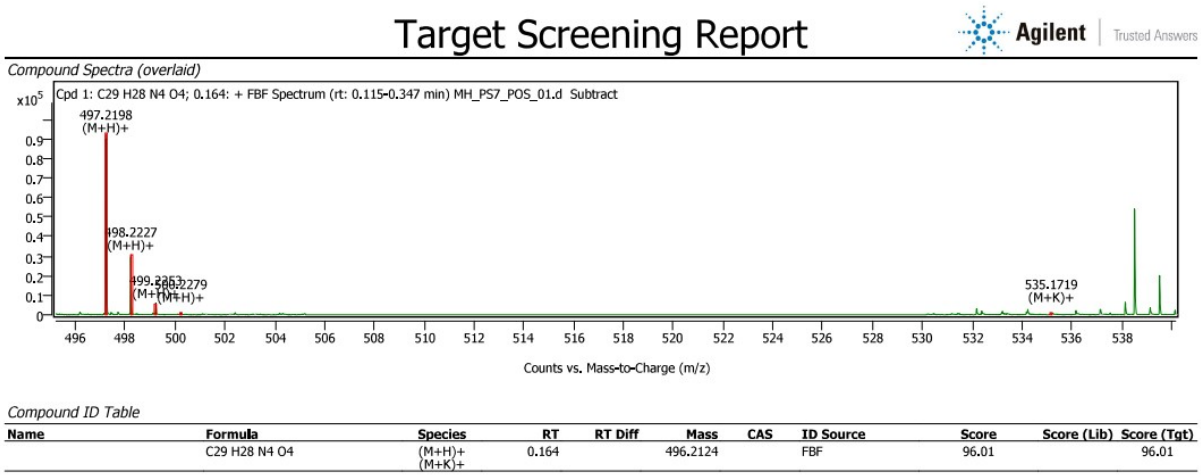

Fig. S3 HRMS spectra of probe **MBH.**

S2: Synthesis procedure of MBA

4,4'-methylenediamine (50 mg, 0.252 mmol) was added to 2-hydroxy-1-napthaldehyde (0.504 mmol, 86.77 mg) in 3 mL of MeOH with the following addition of a catalytic amount of acetic acid and then refluxed for 7 h. TLC was used to monitor the progress of the reaction. After condensation, the reaction mixture was cooled, and a deep yellow-colored solid was filtered and washed systematically with MeOH, after which it was dried in a desiccator. Yield: 92%

Characterizations: ^{1}H NMR (400 MHz, DMSO-d_6, 25 °C) δ(ppm): 15.88 s, (1H, -OH), 9.62 s, (1H, -CH=N), 8.47 d, (2H), 7.92 d, (1H), 7.79 d, (1H), 7.55 t, (1H), 7.35 t, (1H), 7.30 d, (1H), 6.99 d, (1H), 6.91 d, (1H), 6.52 d, (1H), 3.79 s, (1H) (**Fig. S4**). ^{13}C NMR (100 MHz, δ (ppm) DMSO-d_6): 173.56, 157.33, 149.29, 143.75, 139.44, 135.85, 132.33, 131.84, 131.67, 130.74, 129.23, 126.06, 125.04, 123.05, 116.78, 111.03 (**Fig. S5**) and the mass spectra m/z is found to be 507.2085 (**Fig. S6**) confirming the formation of our **MBA.**

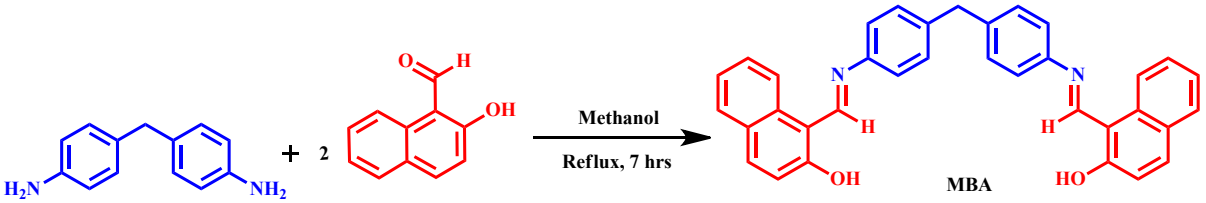

Scheme S2: Synthetic procedure of our desired probe **MBA.**

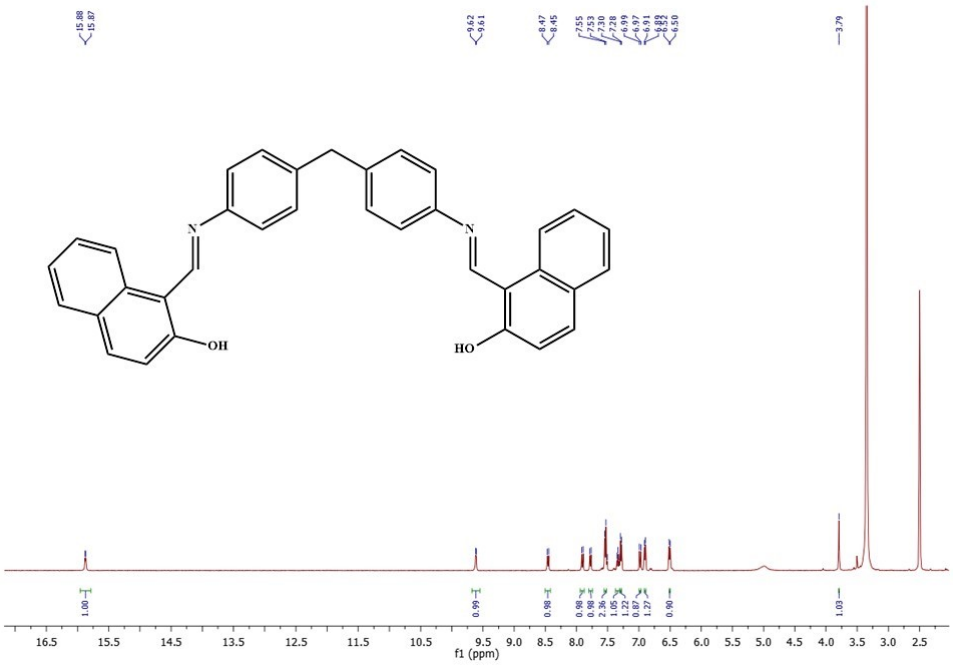

Fig. S4 ^{1}H NMR of probe **MBA.**

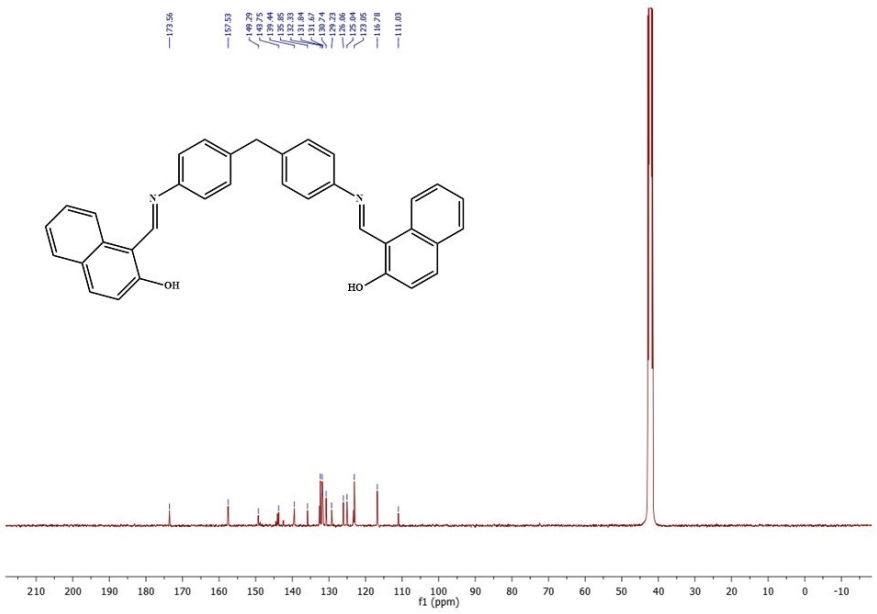

Fig. S5 ^{13}C NMR of probe **MBA.**

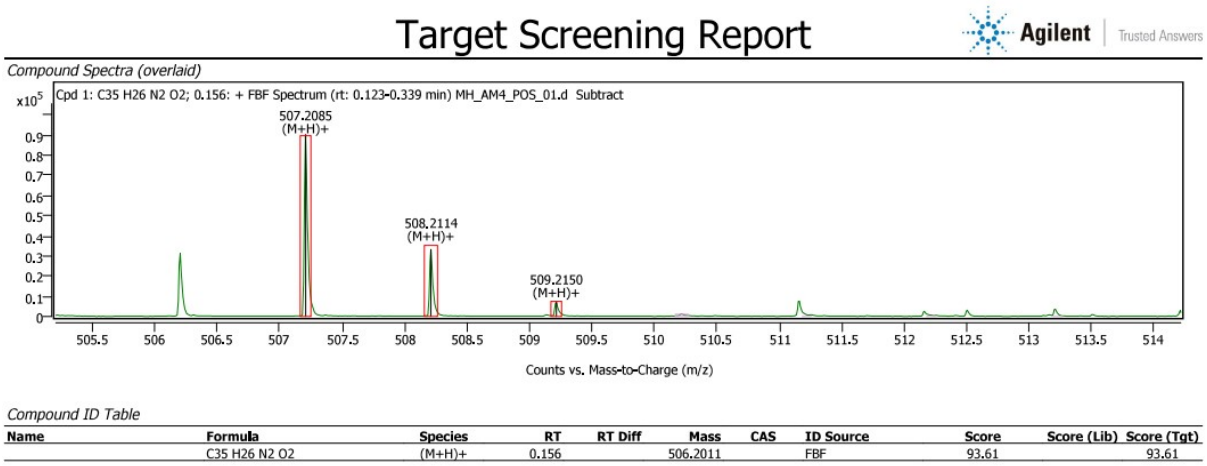

Fig. S6 HRMS spectra of probe **MBA.**

S3: Synthesis procedure of MBB

4,4'-methylenediamine (50 mg, 0.252 mmol) was added to 2-hydroxbenzaldehyde (0.504 mmol, 61.55 mg) in 3 mL of MeOH with the following addition of a catalytic amount of acetic acid and then refluxed for 8 h. TLC was used to monitor the progress of the reaction. After condensation, the reaction mixture was cooled, and a light yellow-colored solid was filtered and washed systematically with MeOH, after which it was dried in a desiccator. Yield: 94%

Characterizations: ^{1}H NMR (400 MHz, DMSO-d_6, 25 °C) δ(ppm): 13.16 s, (1H, -OH), 8.94 s, (1H, -CH=N), 7.64 d, (1H), 7.42 d, (1H), 7.38 t, (1H), 6.99 t, (1H), 4.02 s, (1H) (**Fig. S7**). ^{13}C NMR (100 MHz, δ (ppm) DMSO-d_6): 163.46, 160.74, 146.52, 140.67, 133.64, 132.98, 130.23, 129.67, 121.98, 119.59, 117.04, 70.24 (**Fig. S8**) and the mass spectra m/z is found to be 407.1779 (**Fig. S9**) confirming the formation of our **MBB.**

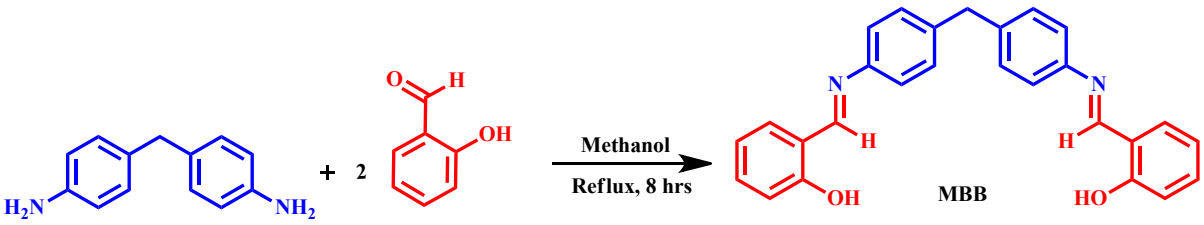

Scheme S3: Synthetic procedure of our desired probe **MBB.**

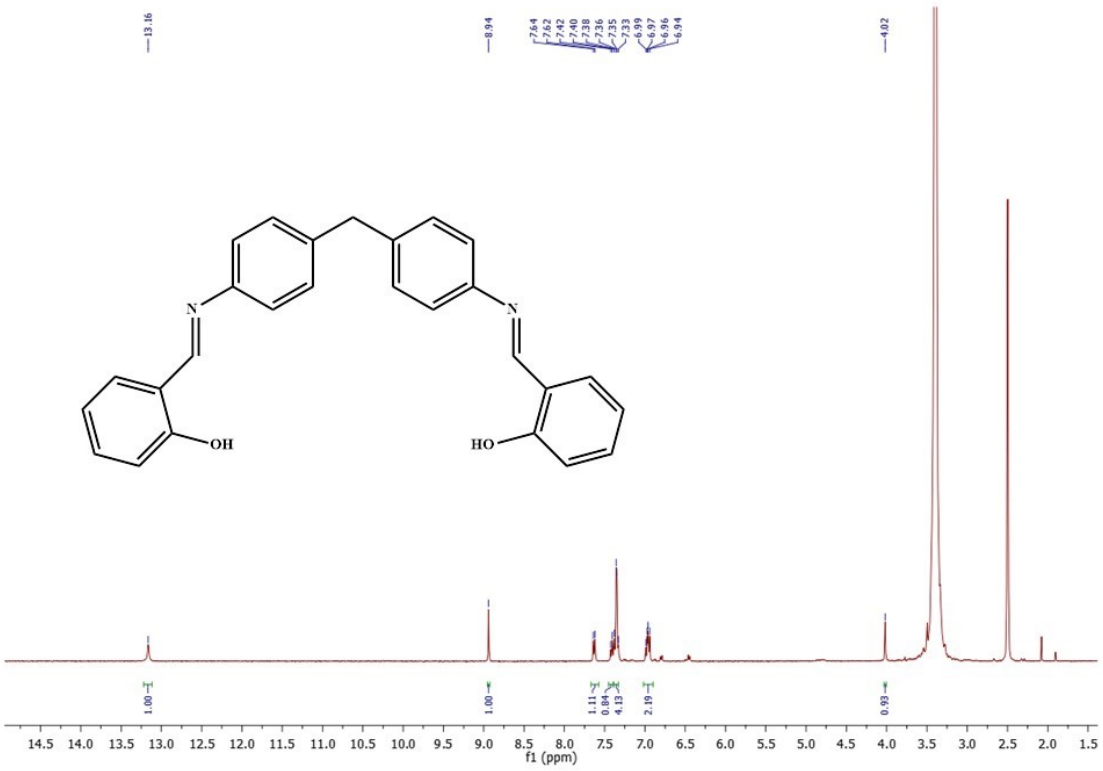

Fig. S7 ^{1}H NMR of probe **MBB.**

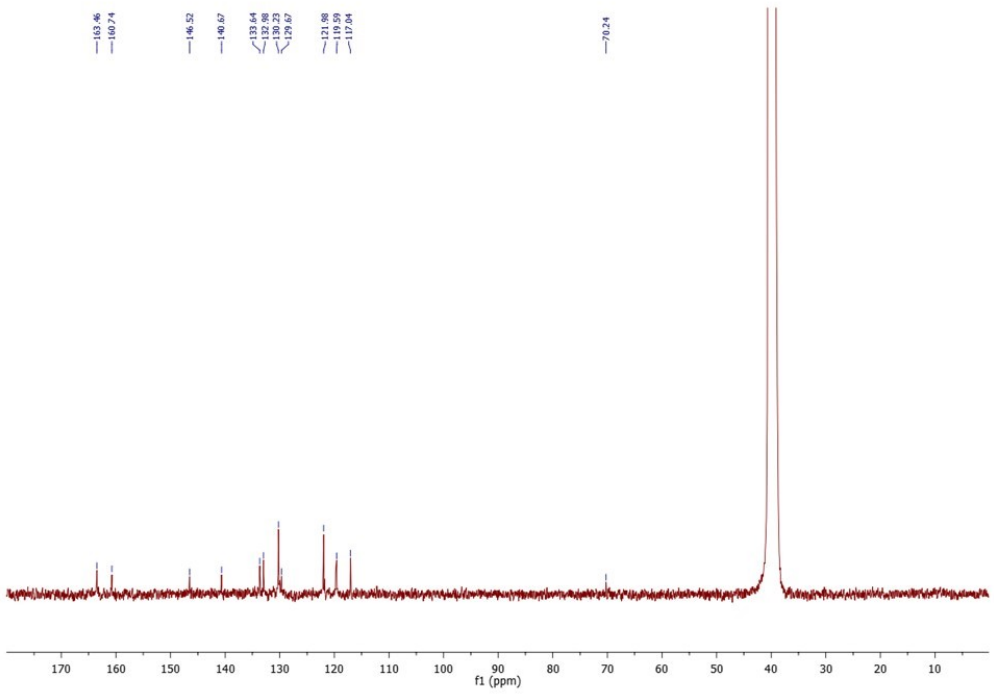

Fig. S8 ^{13}C NMR of probe **MBB.**

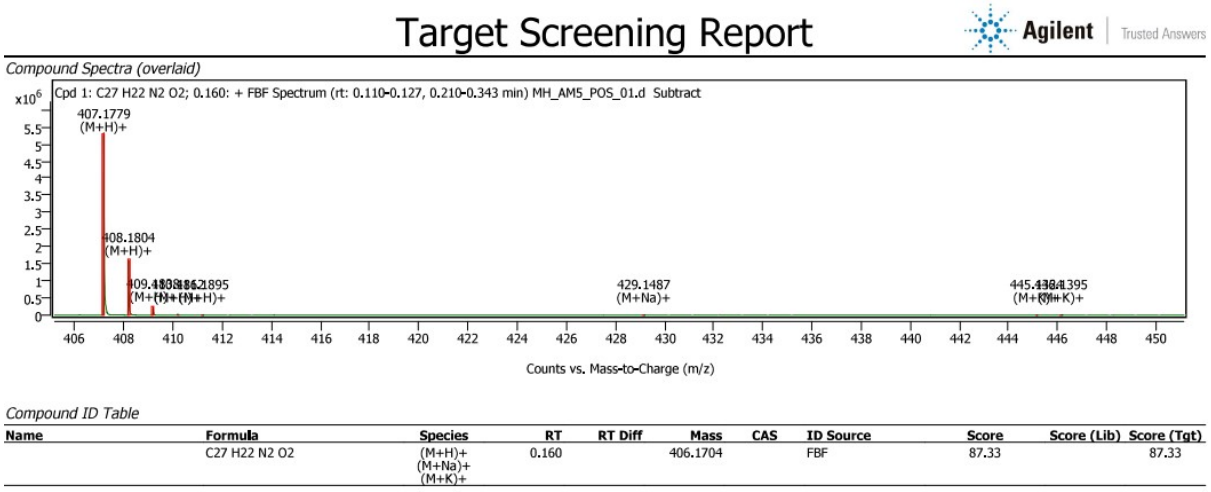

Fig. S9 HRMS spectra of probe **MBB.**

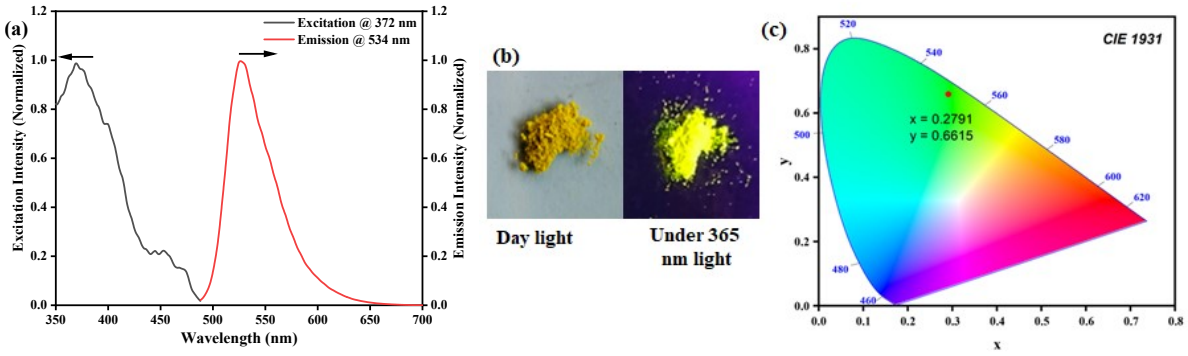

Fig. S10 (a) Excitation and emission spectra of our developed probe **MBB (b)** photograph of our neat probe in daylight (left) and under UV light 365 nm (right). **(c)** Corresponding color chromaticity diagram of our neat solid probe.

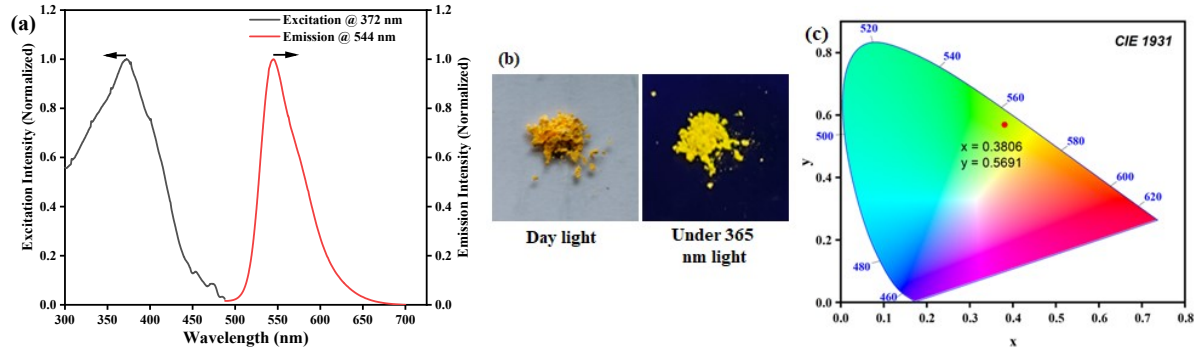

Fig. S11 (a) Excitation and emission spectra of our developed probe **MBH (b)** photograph of our neat probe in daylight (left) and under UV light 365 nm (right). **(c)** Corresponding color chromaticity diagram of our neat solid probe.

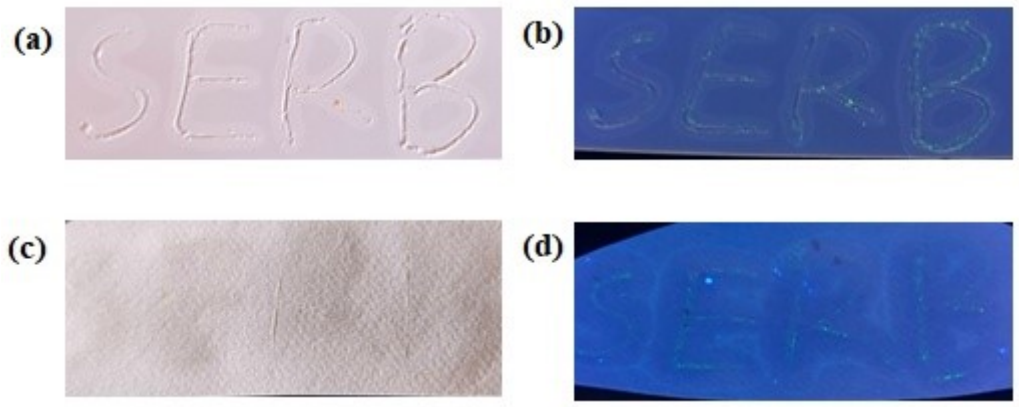

Fig. S12 Visibility of the SERB letter, written by neat probe **MBA** in daylight **(a) (c)** and under UV light 365 nm **(b) (d)** on the surface off TLC plate and Whatman-41 filter paper.

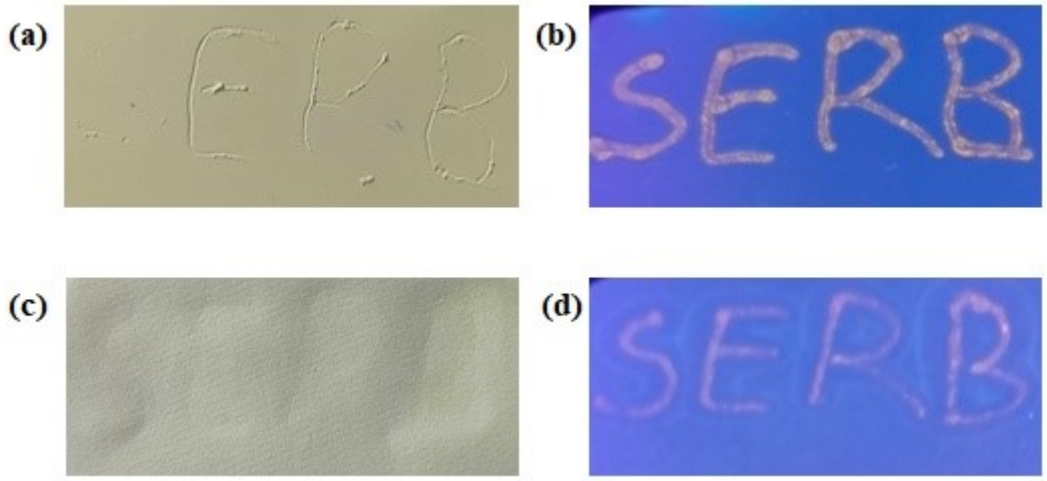

Fig. S13 Visibility of the SERB letter, written by neat probe **MBH** in daylight **(a) (c)** and under UV light 365 nm **(b) (d)** on the surface off TLC plate and Whatman-41 filter paper.

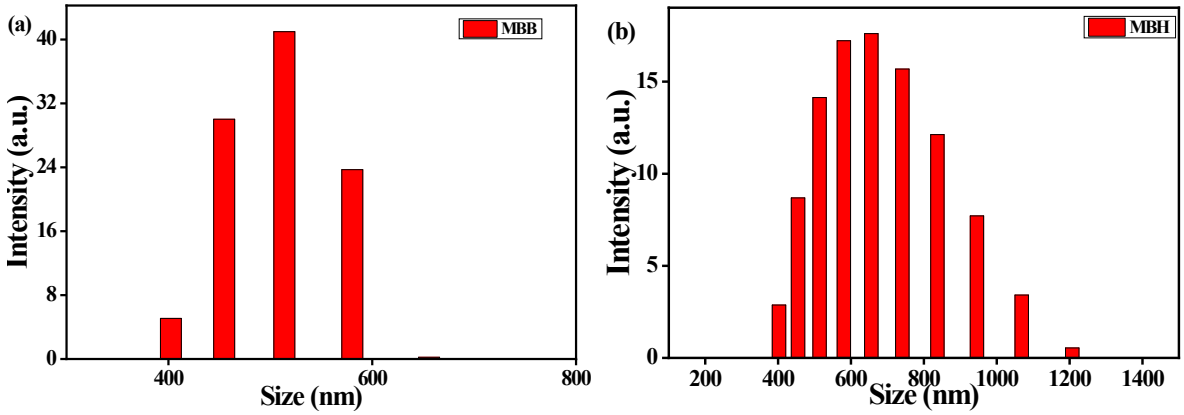

Fig. S14 Dynamic light scattering (DLS) spectrum of probe (a) **MBB**, (b) **MBH**

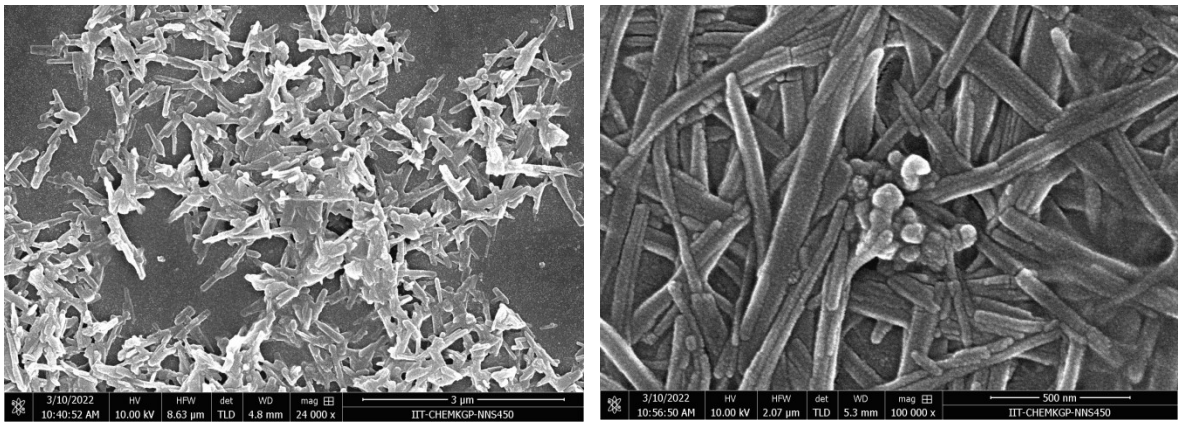

Fig. S15 SEM images of the fabricated low dimensional particle of our probe **MBB** (left) and **MBH** (right).

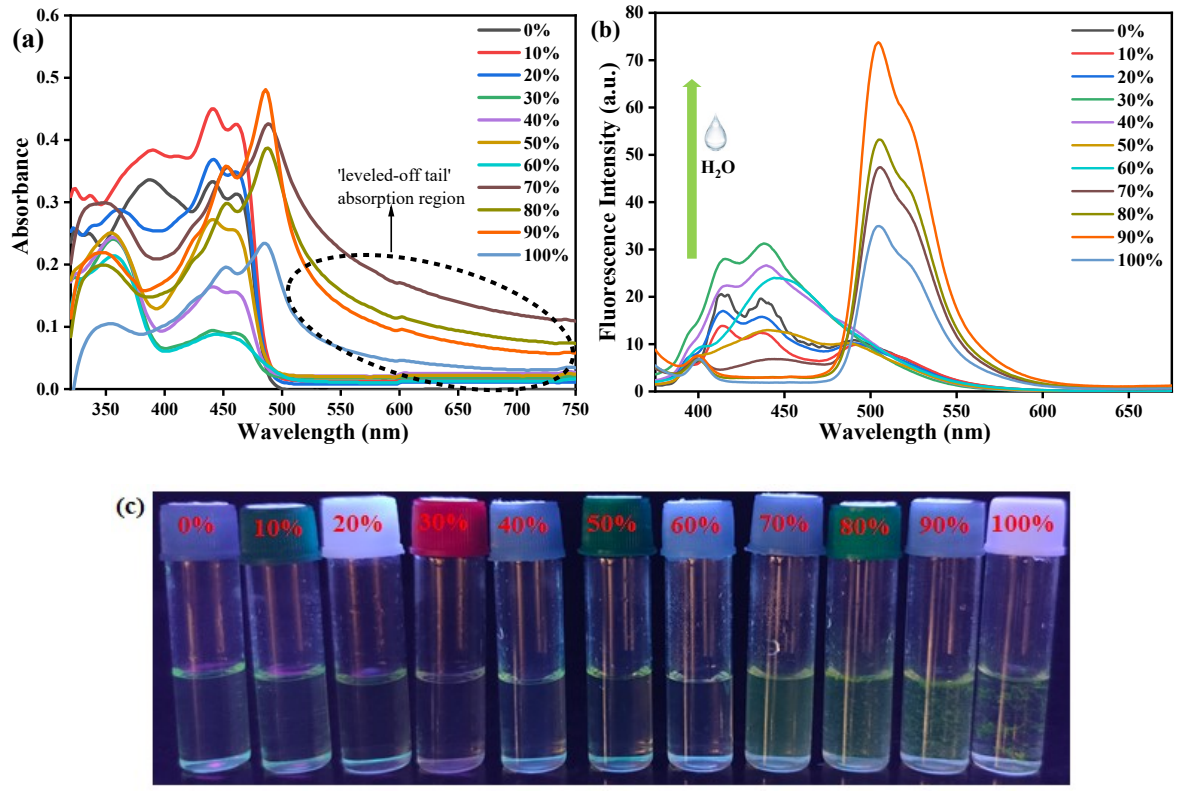

Fig. S16 (a) Changes in the absorbance spectrum of **MBA** upon increasing the water percentage in DMSO (from 0% to 100%). **(b)** Emission spectra of **MBA** in increasing aqueous medium (from 0% to 100%). **(c)** Pictorial presentation of nanoparticles formation upon increasing volume of water.

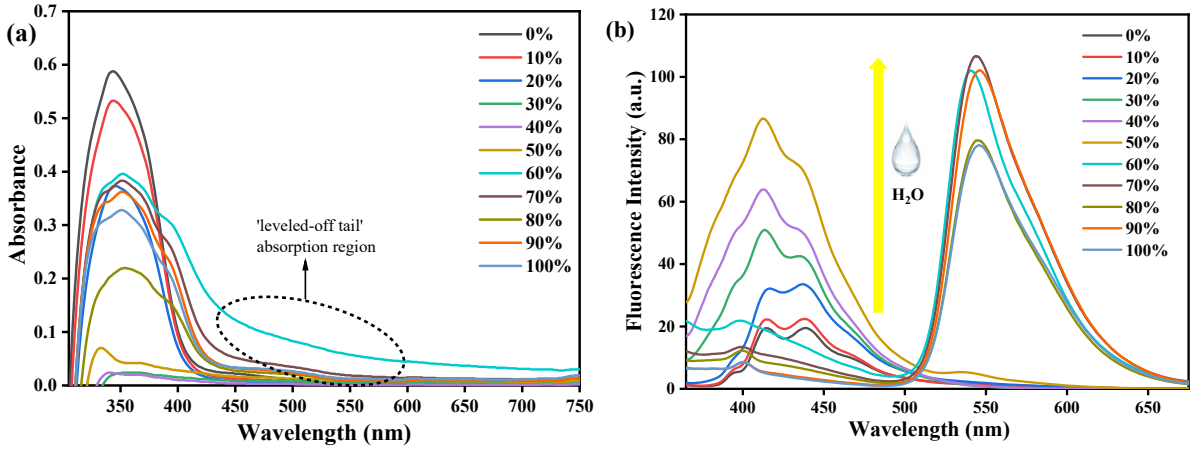

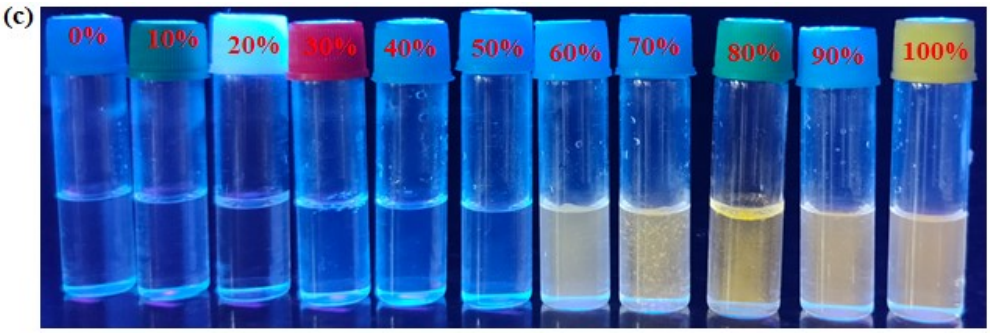

Fig. S17 (a) Changes in the absorbance spectrum of **MBH** upon increasing the water percentage in DMSO (from 0% to 100%). **(b)** Emission spectra of **MBH** in increasing aqueous medium (from 0% to 100%). **(c)** Pictorial presentation of nanoparticles formation upon increasing volume of water.

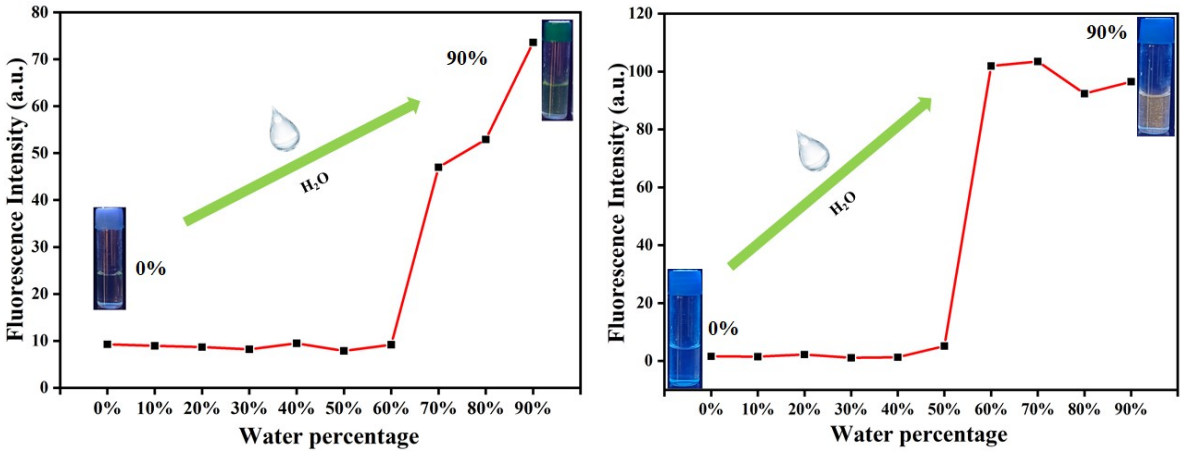

Fig. S18 Emission intensity changes of probe **MBA** (left) and **MBH** (right) in DMSO/H_2O mixture upon difference water percentages Inset: pictorial change of 0% water (colorless) and 90% water (green and yellow color) under UV light (365 nm).

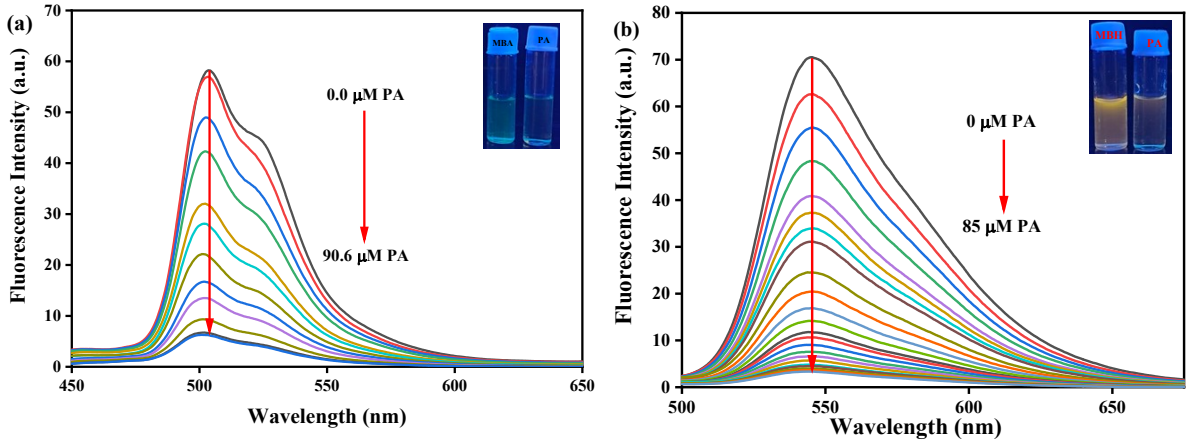

Fig. S19 Altering the fluorescence spectra (λ_{ex} = 350 nm) of a fluorescent **MBA** & **MBH** aggregate (comprising 99% water) while introducing the various concentrations of PA.; Inset: visualize color changes observation from **(a)** strong green & **(b)** yellow color to non-fluorescent colorless in the attendance of PA.

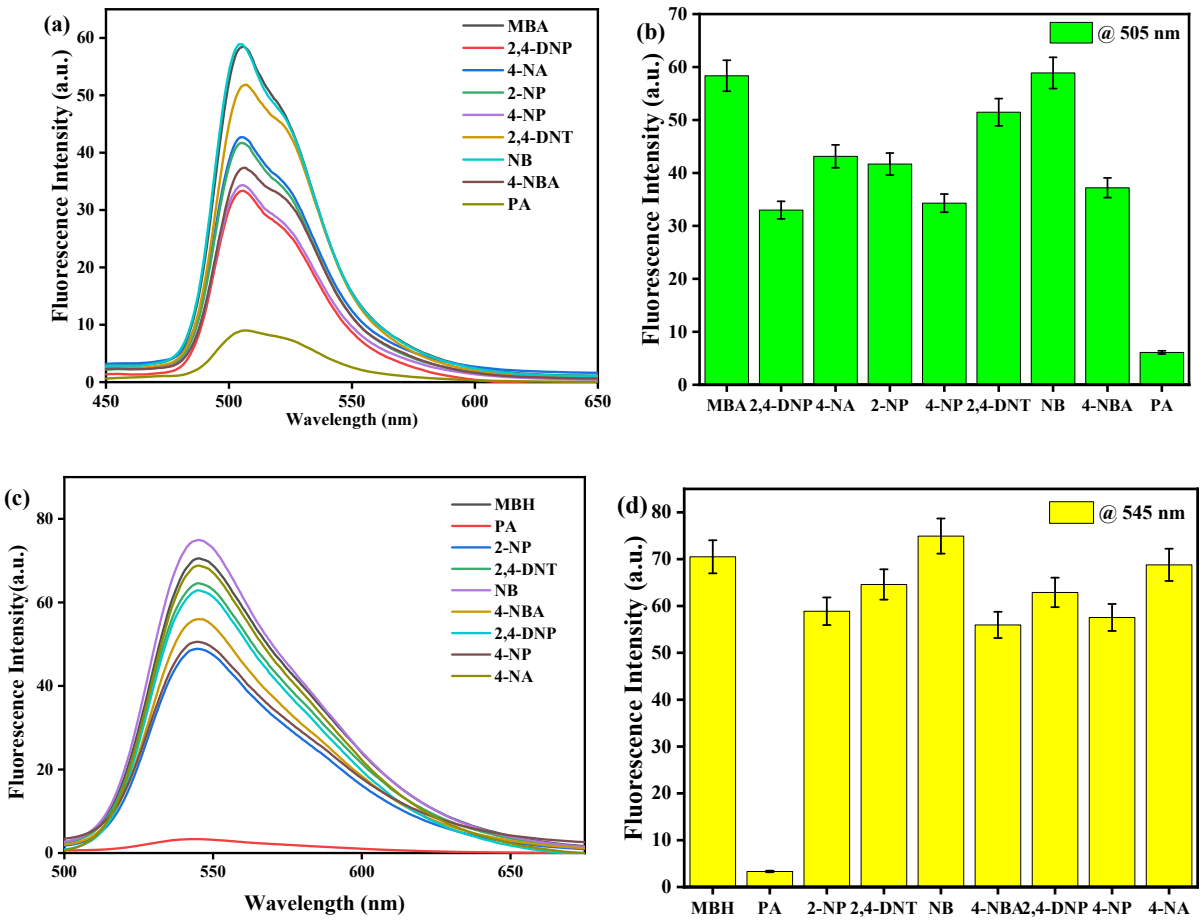

Fig. S20 Emission spectra (λ_{ex} = 350 nm) of **(a) MBA (c) MBH** microparticles with several nitro aromatics compounds. Bar plot of fluorescence quenching of **(b) MBA (d) MBH** microparticles after the addition of various nitroaromatic compounds.

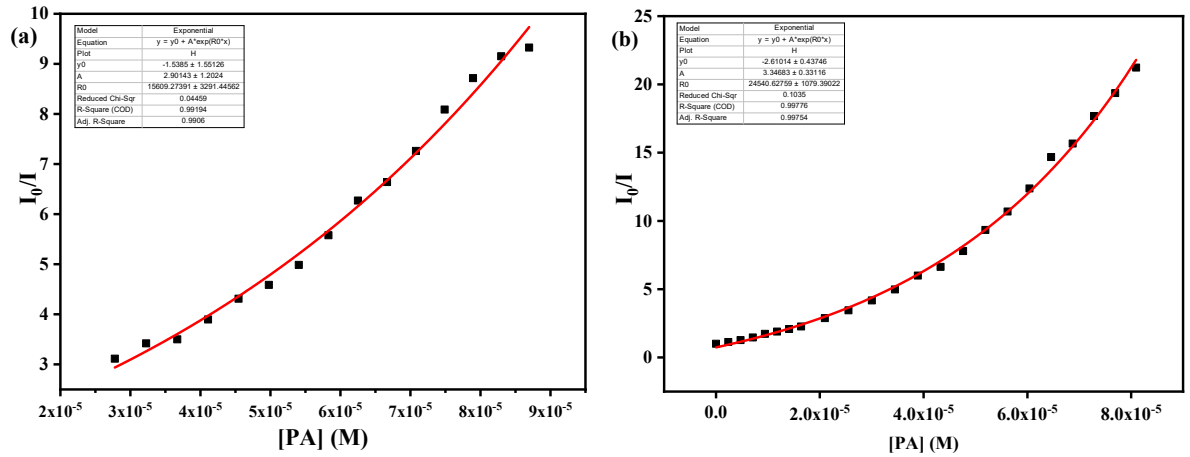

Fig. S21 Stern-Volmer plot of the quenching of aggregated **(a) MBA** and **(b) MBH** on interaction with the PA.

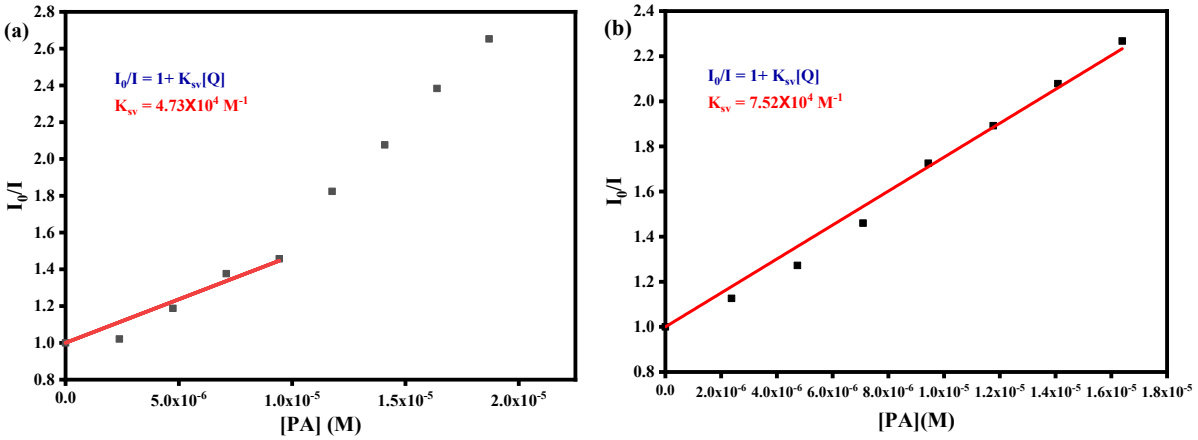

Fig. S22 Linear plot for the calculation of dynamic quenching constant (a) **MBA** and (b) **MBH**.

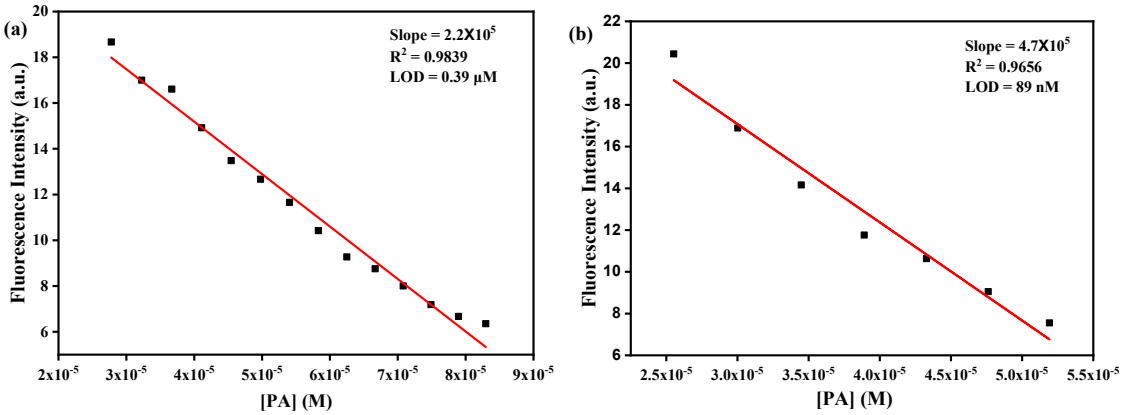

Fig. S23 The linear calibrations plot the [PA] vs. photoluminosity to estimate the LOD value for the recognition of PA ions utilizing microparticles of (a) **MBA** and **(b) MBH**, respectively.

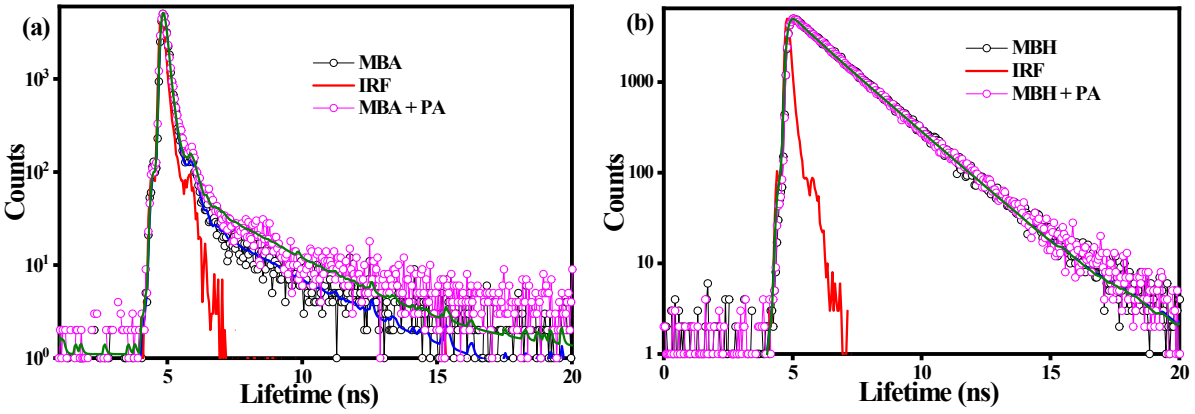

Fig. S24: Fluorescence lifetime decay profile of **(a) MBA** and **(b) MBH** aggregated in the absence and presence of PA.

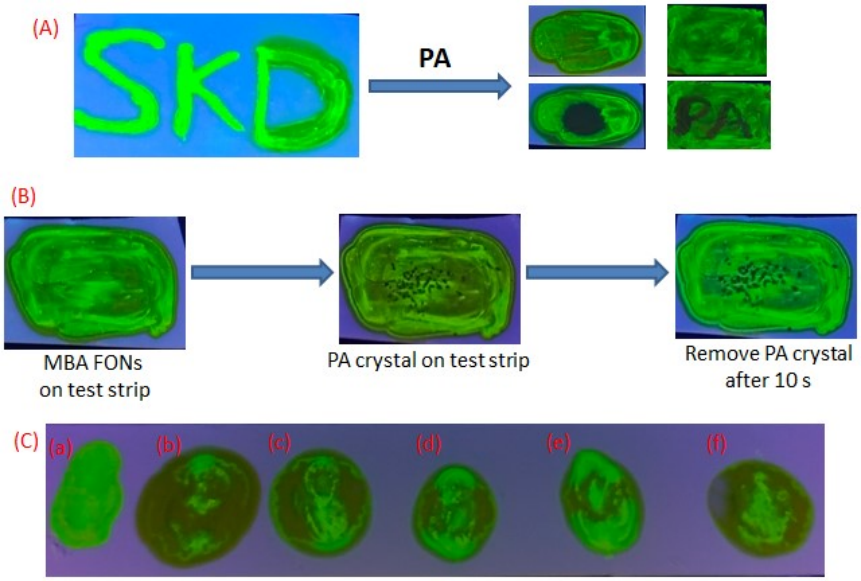

Fig. S25 (A) Pictorial representation of **MBA** microparticles absorbed test strip before and after addition of PA. (**B**) Fluorescence image of PA crystal on the test strip and remove PA crystal after 10 s. (**C**) Fluorescence test strip image after the introduction of various concentrations of PA (a) **MBA** microparticles, (b) 10^{-3}, (c) 10^{-4}, (d) 10^{-5}, (e) 10^{-6}, (f) 10^{-7}.

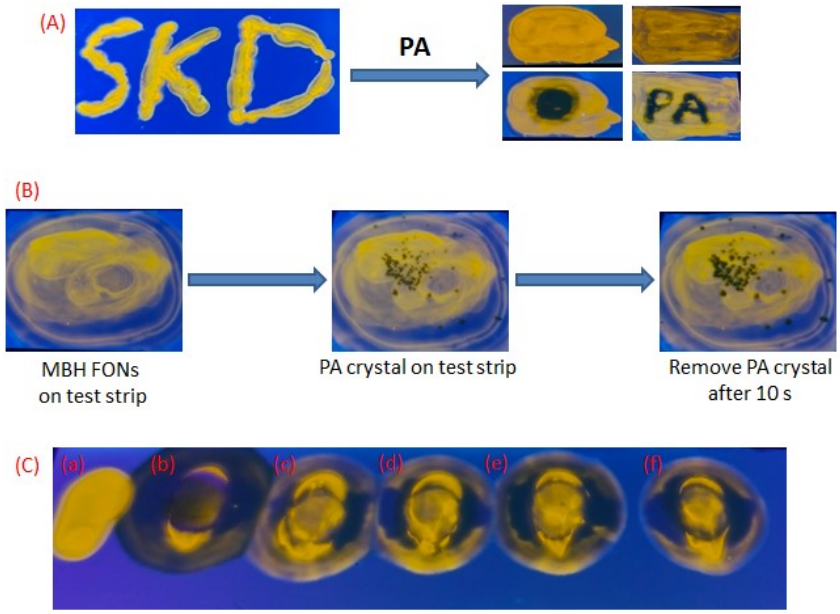

Fig. S26 (A) Pictorial representation of **MBH** microparticles absorbed test strip before and after addition of PA. (**B**) Fluorescence image of PA crystal on the test strip and remove PA crystal after 10 s. (**C**) Fluorescence test strip image after the introduction of various concentrations of PA (a) **MBH** microparticles, (b) 10^{-3}, (c) 10^{-4}, (d) 10^{-5}, (e) 10^{-6}, (f) 10^{-7}.

Table S1: Comparison of the detection limit, and the solvent used for the detection of PA by various chemosensors.

Sl. No	Sensor	Solvent	LOD	Ref.
1	**Methylenediamine based**	**90% water-DMSO**	**5.97 nM, 0.39 µM, 89 nM**	**Current work**
2	Neutral red	ACN	0.639 µM	1
3	Dabsyl derivative	ACN	7.2 µM	2
4	((E)-2-(4-(bis(pyrin-2-ylmethyl)amino)styryl)-3-ethylbenzo[d]thiazol-3-ium iodide)	ACN	1.59 µM	3
5	Thiophene based probe	THF	5.7 µM	4
6	FRET-based rhodamine derivative	Ethanol	0.820 µM	5
7	Zr(IV) based MOF	Methanol	1.63 µM	6
8	9-Anthracenecarboxamide appended probes (1-3)	Ethanol	1 µM	7
9	(E)-4-(2-(pyridin-4-	THF	1.75 µM	8

	yl)vinyl)aniline			
10	unsymmetrical boron detonate complexes	Dichloromethane ($CHCl_2$)	21.5 μM	[9]
11	Lanthanide-based coordination polymer	Chloroform	98 μM	[10]
12	Microporous polymer based on fluorescein	THF	0.722 μM	[11]
13	1,3,5-tris(4'-(N,N-dimethylamino)phenyl)benzene	ACN	6.55 μM	[12]
14	2,6-Divinylpyridine-appended anthracene derivative	THF	2.184 μM	[13]
15	1- imidazolyl methyl pyrene-based sensor	Toluene	2.515 μM	[14]
16	dodecylbenzene-sulfonic acid (DBSA)-doped polyaniline	N-Methyl-2-pyrrolidone	1.00 μM	[15]
17	anthracene-functionalized fluorescent tris-imidazolium sensor 1 sensor 2	DMSO	2.039 μM 1.545 μM	[16]
18	meso diamino phenyl 1, 3, 5, 7-tetramethyl BODIPY dye	CH_3CN	NA	[17]
19	tetraphenyl calix[4]arene	THF	1.54 μM	[18]
20	Tb-based MOF	Methanol	NA	[19]
21	δ ,ɤ-unsaturated β-ketothiolester	THF	16 μM	[20]
22	AIE-based azine derivatives	THF	26 μM	[21]
23	Perylene diimide probes	DMF	1.0 μM	[22]
24	2-arylbenzothiazoles derivatives	Chloroform	21.6 μM 19.0 μM	[23]

References

1 P. Sarkar, N. Tohora, M. Mahato, S. Ahamed, T. Sultana and S. K. Das, *J. Fluoresc.*, 2023, **1**, 1–17.

2 P. Kumar, D. Arya, D. Nain, A. Singh, A. Ghosh and D. A. Jose, *Dye. Pigment.*, 2019, **166**, 443–450.

3 A. Ghosh, S. K. Seth, A. Ghosh, P. Pattanayak, A. Mallick and P. Purkayastha, *Chem. – An Asian J.*, 2021, **16**, 1157–1164.

4 X. Lu, G. Zhang, D. Li, X. Tian, W. Ma, S. Li, Q. Zhang, H. Zhou, J. Wu and Y. Tian,

Dye. Pigment., 2019, **170**, 107641.

5 E. Zhang, P. Ju, P. Guo, X. Hou, X. Hou, H. Lv, J. J. Wang and Y. Zhang, *RSC Adv.*, 2018, **8**, 31658–31665.

6 M. Sk and S. Biswas, *CrystEngComm*, 2016, **18**, 3104–3113.

7 A. Pandith, A. Kumar, J. Y. Lee and H. S. Kim, *Tetrahedron Lett.*, 2015, **56**, 7094–7099.

8 J. Pan, F. Tang, A. Ding, L. Kong, L. Yang, X. Tao, Y. Tian and J. Yang, *RSC Adv.*, 2014, **5**, 191–195.

9 S. Sriram Babu and S. Shanmugam, *J. Mater. Chem. C*, 2017, **5**, 4788–4796.

10 S. Srivastava, B. K. Gupta and R. Gupta, *Cryst. Growth Des.*, 2017, **17**, 3907–3916.

11 T. M. Geng, S. N. Ye, Y. Wang, H. Zhu, X. Wang and X. Liu, *Talanta*, 2017, **165**, 282–288.

12 P. Vishnoi, S. Sen, G. N. Patwari and R. Murugavel, *New J. Chem.*, 2015, **39**, 886–892.

13 D. C. Santra, M. K. Bera, P. K. Sukul and S. Malik, *Chem. – A Eur. J.*, 2016, **22**, 2012–2019.

14 R. Sodkhomkhum, M. Masik, S. Watchasit, C. Suksai, J. Boonmak, S. Youngme, N. Wanichacheva and V. Ervithayasuporn, *Sensors Actuators B Chem.*, 2017, **245**, 665–673.

15 V. Lakshmidevi, C. V. Yelamaggad and A. Venkataraman, *ChemistrySelect*, 2018, **3**, 2655–2664.

16 B. Roy, A. K. Bar, B. Gole and P. S. Mukherjee, *J. Org. Chem.*, 2013, **78**, 1306–1310.

17 Y. Erande, S. Chemate, A. More and N. Sekar, *RSC Adv.*, 2015, **5**, 89482–89487.

18 S. K. Dinda, M. A. Hussain, A. Upadhyay and C. P. Rao, DOI:10.1021/acsomega.9b02855.

19 P. Ju, E. Zhang, L. Jiang, Z. Zhang, X. Hou, Y. Zhang, H. Yang and J. Wang, *RSC Adv.*, 2018, **8**, 21671–21678.

20 S. S. Babu and S. Shanmugam, *ChemistrySelect*, 2018, **3**, 4075–4081.

21 M. Sathiyaraj, K. Pavithra and V. Thiagarajan, *New J. Chem.*, 2020, **44**, 8402–8411.

22 P. S. Hariharan, J. Pitchaimani, V. Madhu and S. P. Anthony, *J. Fluoresc.*, 2016, **26**, 395–401.

23 S. Chaudhary, H. Sharma and M. D. Milton, *ChemistrySelect*, 2018, **3**, 4598–4608.